In-silico quest for bactericidal but non-cytotoxic nanopatterns

Mirzaali Mazandarani, Mohammad; Van Dongen, I. C.P.; Tümer, N.; Weinans, H.; Yavari, S. Amin; Zadpoor, A. A.

DOI
10.1088/1361-6528/aad9bf

Publication date
2018

Document Version
Accepted author manuscript

Published in
Nanotechnology

Communication

In-silico quest for bactericidal but non-cytotoxic nanopatterns

M. J. Mirzaali[a], I.C.P. van Dongen[a,b], N. Tümer[a], H. Weinans[a,b,c], S. Amin Yavari[b,*,1], A. A. Zadpoor[a,1]

[a] *Department of Biomechanical Engineering, Faculty of Mechanical, Maritime, and Materials Engineering, Delft University of Technology (TU Delft), Mekelweg 2, 2628 CD, Delft, The Netherlands*

[b] *Department of Orthopedics, University Medical Centre Utrecht, Utrecht, The Netherlands*

[c] *Department of Rheumatology, University Medical Centre Utrecht, Utrecht, The Netherlands*

[1] Both authors share last authorship

[*] Corresponding author

E-mail address: s.aminyavari@umcutrecht.nl, saber.aminyavari@gmail.com

Abstract

Nanopillar arrays that are bactericidal but not cytotoxic against the host cells could be used in implantable medical devices to prevent implant-associated infections. It is, however, unclear what heights, widths, interspacing, and shape should be used for the nanopillars to achieve the desired antibacterial effects while not hampering the integration of the device in the body. Here, we present an *in-silico* approach based on finite element modeling of the interactions between *Staphylococcus aureus* and nanopatterns on the one hand and osteoblasts and nanopatterns on the other hand to find the best design parameters. We found that while the height of the nanopillars seems to have little impact on the bactericidal behavior, shorter widths and larger interspacings substantially increase the bactericidal effects. The same combination of parameters could, however, also cause cytotoxicity. Our results suggest that a specific combination of height (120 nm), width (50 nm), and interspacing (300 nm) offers the bactericidal effects without cytotoxicity.

Keywords: Nanopattern design, implant-associated infections, osseointegration, finite element modelling.

Nanopillar arrays found on the wings of cicada and dragonfly behave as natural bactericidal surfaces [1]. The nanopillars penetrate into the bacterial walls or stretch them, resulting in cytoplasm leakage and cell death [2]. The nanopillars found on the wing of cicada have a height of 200 nm, a nanopillar interspacing of 170 nm, a width at the base of 100 nm, and a width at the cap of 60 nm [3]. Similar nanopatterned structures could be found on the wings of dragonfly with heights of 189-311 nm and widths of 37-57 nm [2]. Surfaces decorated with similar types of nanopatterns have been fabricated by researchers and are demonstrated to exhibit bactericidal behavior [4], [5].

Implantable medical devices could potentially be covered with such types of nanopatterns to protect patients against implant-associated infections (IAIs). In the case of orthopaedic implants, IAIs are one of the major factors limiting the longevity of implants [6], [7]. For example, 0.5-5% of the patients undergoing joint replacement surgeries experience IAIs [8]. Many researchers are therefore developing coatings [9], surface treatments [10], [11], and hydrogels [12] to prevent the infections associated with orthopaedic surgeries. However, many of these coatings may elicit undesired effects such as cytotoxicity [13]. In comparison, nanopatterned surfaces offer a safer non-pharmaceutical alternative that could be harnessed to prevent IAIs.

A major research question when designing antibacterial nanopatterns is: ‘what are the best values for the height, diameter, and inter-spacing of the nanopillars such that the nanopatterns are bactericidal but not cytotoxic against host cells?’ Answering this question requires a systematic study of how different parameters influence both types of behaviors. The major challenge when performing such studies is accurate and reproducible fabrication of nanopatterns with different sets of design parameters. Nanoimprint lithography [14],

nanowires based on hydrothermal treatment [15], or deep reactive ion etching [16] have been currently in use for fabrication of nanopatterns. Most of these techniques are, however, costly, slow, and labor-intensive and need much calibration before they could be applied to new (metallic) materials. Here, we present an *in-silico* approach based on computational modeling of the cell-surface interactions to find the design parameters of nanopatterns.

We used a model of Gram-positive *Staphylococcus aureus* (*S. aureus*), which is a common bacterium in the human body and a major cause of bone and joint infections [17], to study the response of bacteria to nanopatterns. Osteoblasts are responsible for *de novo* bone formation and osseointegration of the implants [11]. Therefore, these cells were used for the simulations to study their response to nanopatterns with the goal to preserve them, i.e. no cytotoxicity behavior.

S. aureus is spherical in shape with a relatively thick wall consisting of peptidoglycans, which give the bacteria its shape and strength [18] (Figure 1a). The geometrical dimensions of the bacterial cell, i.e. the outer diameter ($D = 600$ nm) and thickness ($th = 10$ nm), were set according to the information available in the literature [19], [20]. Osteoblasts were modelled using polygons with a hat-shape for the cytoplasm and an ellipse shape for the nucleus (Figure 1a). The maximum diameter of the cytoplasm ($D = 20$ µm) and its thickness ($th = 6$ nm) as well as the dimensions of the nucleus (Figure 1a) were chosen based on the values reported in the literature [21], [22].

A visco-hyperelastic material model (Neo-Hookean, viscoelastic) was used for modeling the cytoplasm of *S. aureus* [23], [24], while the cell wall was assumed to behave linear elastically [25], [26]. A linear elastic material model was used for modeling the nucleus and membrane of the osteoblast cells [22] and a similar visco-hyperelastic material model similar to the one

used for *S. aureus* was used for the modeling the cytoplasm of osteoblasts [21], [22], [24]. *An analysis of the time period for the viscoelastic material properties was discussed in the supplementary document and Figure S1.* A summary of all parameters and their sources are presented in Table S1. A linear elastic material model ($E = 150$ GPa, $\nu = 0.278$ [27]) was used to describe the mechanical behavior of nanopillars. This was based on the assumption that nanopillar were made using electron beam induced deposition with platinum pre-cursors [28]. *We also considered different material properties for the nanopillars (see the supplementary document, Figure S2).*

We used a nonlinear implicit solver (Abaqus Standard 6.14) to simulate the models. 2D plane strain quadratic quadrilateral elements with hybrid deformation (CPE8H) and without (CPE8) were respectively used for meshing the cells and nanopillars. A mesh convergence analysis was performed (see the supplementary document, *Figure S3, and S4*) according to which a minimum element size of 3 nm and 10 nm were respectively used for modeling the *S. aureus* and osteoblast cells. An out-of-plane thickness of 600 nm and 20 μm were considered in the modeling of *S. aureus* and osteoblast cell, respectively.

The finite element models simulated the conditions used in an *in vitro* experimental study of how bacteria interact with nanopatterned surfaces [29]. We assumed that cells experience two types of forces including their own weight and the forces caused by the height of the water (culture medium) column. The sum of both forces was applied as a body force. The buoyant forces were small in comparison and were, thus, neglected.

A variation of the height, H, width, W, interspace, IS, radius, r, and shape of the nanopatterned surfaces (Figure 1b) were used in the finite element models. To evaluate the effects of each design parameter on the deformation of cell walls/ membrane, the most

extreme values of each parameter found in the literature were implemented in the finite element models. For example, the smallest and largest values considered for the width, W, were respectively 25 nm and 200 nm [11], [14], [16], [30].

A total mass of 1 pg was used for *S. aureus* [31]. A parametric study showed that the obtained overall stress/strain distributions are in general similar regardless of how the mass is distributed between the cell wall and cytoplasm (see the supplementary document for the details, *Figure S5*). We therefore assumed that the cytoplasm and cell walls equally contribute to the mass of the bacteria, applying 50% of the total body force to each compartment. The mass of the osteoblast cell is reported to be around 1.48 ng with different densities for its constituents, i.e., $\rho_{\text{nucleus}} = 1.8\times10^{-9}$ [ton/mm^3], $\rho_{\text{cytoplasm}} = 1.5\times10^{-9}$ [ton/mm^3], and $\rho_{\text{membrane}} = 0.6\times10^{-9}$ [ton/mm^3] [21], [22]. The body forces applied to the different parts of the cell models were determined accordingly (Table S2).

A nonlinear surface-to-surface contact type was considered for all the simulations with a rough frictional formulation for the tangential behavior and hard contact pressure-overclosure for the normal behavior. The contact type used enabled a smooth sliding of the cells into the area between the nanopillars. The different compartments of the cells were tied to each other. A strain-based failure criterion was used to predict a rupture in the cell wall (or membrane) of bacteria (or host cells). The bacteria and host cells were assumed to be killed if numerically calculated equivalent von Mises strain, ε_{eq}, in the cell wall or membrane exceeded threshold of $\varepsilon_{th} = 0.5$ for *S. aureus* [32] and $\varepsilon_{th} = 1.05$ for osteoblast [33]. Furthermore, sinking depth ratio, SD/D, was defined as the maximum of deformation in the cell wall or membrane, SD, normalized to the diameter of the bacteria or cell, D.

The height of nanopillars did not substantially change the maximum equivalent strain experienced by the cell wall of the bacteria, meaning that height does not influence the bactericidal behavior of the nanopatterns (Figure 2a). However, a combination of the width and interspacing of the nanopillars caused high levels of variation in the maximum equivalent strain induced in the cell wall (Figure 2b, c). The von Mises strain and normalized sinking depth reached their maximum values when the minimum width was combined with the maximum value of the interspacing, i.e., $IS = 300$ nm and $W = 200$ nm (Figure 2b, c). The effects of nanopillar shape on the equivalent von Mises strain were relatively limited (Figure 2d). Smaller values of the relative radius, r/W, caused higher levels of von Mises strain (Figure 2e). *Change in the maximum stress of bacteria and the average stress in nanopillars are shown in Figure S6 of the supplementary document.*

The nanopillar designs that caused high equivalent von Mises strains in the bacteria cell wall were chosen to simulate their interactions with osteoblasts. We found that combining the largest values of nanopillar interspacing with the smallest widths could also result in cytotoxicity (Figure 3a-c). *Change of stress in the osteoblast cell and the nanopillars are depicted in Figure S7 of the supplementary document.* Increasing the width of the nanopillars, however, resulted only in bactericidal behavior but no cytotoxicity (Figure 3b and c). Two non-dimensional parameters $\frac{W}{W+IS}$, and $\frac{R}{IS}$ showed strong correlaa tion with the von Mises strain (Figure 3d, e) and may have some value as surrogate parameters when designing bactericidal nanopatterns. Taken together, the results of the current study point towards one specific combination of height, width, and interspacing to ensure the nanopatterns are bactericidal but not cytotoxic, i.e. $W = 50$ nm, and $IS = 300$ nm.

The diameters of the nanopillars for which bactericidal effects are predicted are between 25 nm and 50 nm. These values are within the range of the diameter of nanopatterns that have been shown to be bactericidal against *S. aureus* [34]. These numerically estimated diameters are also comparable with those found for the dragon fly wing (50-70 nm) that are known to be bactericidal against *S. aureus* [34]. Au nanostructured surface with diameters of 50 nm [30] has also been found to kill *S. aureus*, which is in line with our simulation results. In terms of nanopillar interspacing, the values reported in the literature for bactericidal nanopatterns are usually higher than 100 nm and in the range of 150-300 nm [35]. Not much experimental data regarding the cytotoxicity of the above-mentioned nanopatterns is available in the literature. In one study, nanopillar arrays with an interspacing of 300 nm and a small width at the top (triangular shape pillars) reduced the attachment of mammalian cells [36]. These experimental values are comparable to those for which our models predict cytotoxic behavior (i.e. a diameter of 25 nm and an interspacing of 300 nm).

Systematic study of both bactericidal and cytotoxic behaviors is one of the unique properties of the current study. The next step will consist of experiments in which these predicted design values will be used for evaluating their behavior against bacteria and host cells. Although the predictions of our computational models are in line with experimental findings, the more general trends may be only valid within the ranges for which we have actually run the simulations. For example, a nanopillar tip much sharper than those considered here may kill bacteria. Very sharp nanopillars create singularity in elastic simulations and were therefore avoided. Moreover, sharpest nanopillars are almost certain to be also cytotoxic, as the singular strains experienced at the top most probably will exceed the limit allowable for mammalian cells as well. The trend observed here regarding the height of the nanopillars is

only valid when the sinking depth of the bacteria is smaller than the height of the nanopillars in which case the cell does not feel the extra height of the nanopillars. If the sinking depth goes beyond the height of the nanopillars, larger heights are expected to increase the deformation and, thus, the bactericidal behavior.

We changed the mechanical properties of the nanopillars within three orders of magntidue (i.e. 150 GPa to 150 MPa). This spans the properties of a wide range of relevant materials including titanium and hydroxyapateite. These further simulations have been performed for the cases that showed a bactericidal effect, i.e., $W = 25$ *and* $W = 50$ *with* $IS = 300$*. The conclusions regarding the bactericdial behavior and cytocompatibility of the nanopatterns remained unchangged regardless of the elastic modulus used.*

It is worth mentioning that in this study we only focused on the simulation of Gram-positive bacteria (S.aureus) and not Gram-negative ones. S.aureus is a major cause of infections associated with orthopaedic implants. The Gram-positive and Gram-negative bacteria have different membrane compositions. The Gram-positive bacteria have a thicker cell wall (between 20-80 nm) composed of peptidoglycan and teichoic, which makes for a more rigid cell wall as compared to the Gram-negative bacteria that have a thinner outer membrane (8-12 nm) made up of peptidoglycan [38], [39]. Due to these differences, Gram-negative bacteria are chemically tougher than the Gram-positive ones but mechanically Gram-negative bacteria are weaker. Since our comoputational models do not take the chemical interaction of these cells with nanopatterns into account, we believe that the results presented for the Gram-positive bacteria in this study provides an upper bound for both cell types.

In this study, we only considered the gravitational force and the pressure caused by the water column. The adhesion forces between the bacterium and nanopillars [2], [26], [37], [38] and the resulting shear forces were not taken into account. Hydrophilic surface properties have been also proposed as another mechanism affecting the bactericidal properties of nanopatterns [3], [35], which were not studied here. *From our simulations, it is not clear how much these shear forces and mechanisms individually contribute to the fate of cells. However, to have a realistic simulation of cytotoxic/ bactericidal activity, all of these mechanisms should be taken into account. Furthermore, in this study, we only focused on the contact killing mechanism, while neglecting other chemical mechanisms for killing the bacteria.*

In summary, we developed an *in-silico* approach for finding the best design parameters of nanopillar arrays such that the nanopatterns exhibit bactericidal behavior but are not cytotoxic against host cells. Our finite element models predict that the width and interspacing of the nanopillars are the most important parameters influencing the bactericidal behavior of such arrays. We also found a specific combination of width and interspacing, i.e. $W = 50$ nm, and $IS = 300$ nm, that our models predict to be bactericidal but not cytotoxic for host osteoblasts. The proposed nanopatterns can now be tested e.g. on the titanium surface of joint implants to prevent implant infection and not harm bony ingrowth.

Competing Interests

The authors declare that they have no competing interests.

REFERENCES

[1] E. P. Ivanova, J. Hasan, H. K. Webb, V. K. Truong, G. S. Watson, J. A. Watson, V. A. Baulin, S. Pogodin, J. Y. Wang, M. J. Tobin, and others, "Natural bactericidal surfaces: mechanical rupture of Pseudomonas aeruginosa cells by cicada wings," *Small*, vol. 8, no. 16, pp. 2489–2494, 2012.

[2] C. D. Bandara, S. Singh, I. O. Afara, A. Wolff, T. Tesfamichael, K. Ostrikov, and A. Oloyede, “Bactericidal effects of natural nanotopography of dragonfly wing on Escherichia coli,” *ACS applied materials & interfaces*, vol. 9, no. 8, pp. 6746–6760, 2017.

[3] A. Elbourne, R. J. Crawford, and E. P. Ivanova, “Nano-structured antimicrobial surfaces: From nature to synthetic analogues,” *Journal of colloid and interface science*, vol. 508, pp. 603–616, 2017.

[4] J. A. Inzana, E. M. Schwarz, S. L. Kates, and H. A. Awad, “Biomaterials approaches to treating implant-associated osteomyelitis,” *Biomaterials*, vol. 81, pp. 58–71, 2016.

[5] R. Kuehl, P. S. Brunetto, A.-K. Woischnig, M. Varisco, Z. Rajacic, J. Vosbeck, L. Terracciano, K. M. Fromm, and N. Khanna, “Preventing implant-associated infections by silver coating,” *Antimicrobial agents and chemotherapy*, vol. 60, no. 4, pp. 2467–2475, 2016.

[6] A. de Breij, M. Riool, P. H. Kwakman, L. de Boer, R. A. Cordfunke, J. W. Drijfhout, O. Cohen, N. Emanuel, S. A. Zaat, P. H. Nibbering, and others, “Prevention of Staphylococcus aureus biomaterial-associated infections using a polymer-lipid coating containing the antimicrobial peptide OP-145,” *Journal of Controlled Release*, vol. 222, pp. 1–8, 2016.

[7] J. Raphel, M. Holodniy, S. B. Goodman, and S. C. Heilshorn, “Multifunctional coatings to simultaneously promote osseointegration and prevent infection of orthopaedic implants,” *Biomaterials*, vol. 84, pp. 301–314, 2016.

[8] D. Campoccia, L. Montanaro, and C. R. Arciola, “The significance of infection related to orthopedic devices and issues of antibiotic resistance,” *Biomaterials*, vol. 27, no. 11, pp. 2331–2339, 2006.

[9] I. A. van Hengel, M. Riool, L. E. Fratila-Apachitei, J. Witte-Bouma, E. Farrell, A. A. Zadpoor, S. A. Zaat, and I. Apachitei, “Selective laser melting porous metallic implants with immobilized silver nanoparticles kill and prevent biofilm formation by methicillin-resistant Staphylococcus aureus,” *Biomaterials*, vol. 140, pp. 1–15, 2017.

[10] S. Amin Yavari, L. Loozen, F. L. Paganelli, S. Bakhshandeh, K. Lietaert, J. A. Groot, A. C. Fluit, C. Boel, J. Alblas, H. C. Vogely, and others, “Antibacterial behavior of additively manufactured porous titanium with nanotubular surfaces releasing silver ions,” *ACS applied materials & interfaces*, vol. 8, no. 27, pp. 17080–17089, 2016.

[11] S. Dobbenga, L. E. Fratila-Apachitei, and A. A. Zadpoor, “Nanopattern-induced osteogenic differentiation of stem cells–A systematic review,” *Acta biomaterialia*, vol. 46, pp. 3–14, 2016.

[12] S. Bakhshandeh, Z. Gorgin Karaji, K. Lietaert, A. C. Fluit, C. E. Boel, H. C. Vogely, T. Vermonden, W. E. Hennink, H. Weinans, A. A. Zadpoor, and others, “Simultaneous Delivery of Multiple Antibacterial Agents from Additively Manufactured Porous Biomaterials to Fully Eradicate Planktonic and Adherent Staphylococcus aureus,” *ACS applied materials & interfaces*, vol. 9, no. 31, pp. 25691–25699, 2017.

[13] G. Wang, W. Jin, A. M. Qasim, A. Gao, X. Peng, W. Li, H. Feng, and P. K. Chu, “Antibacterial effects of titanium embedded with silver nanoparticles based on electron-transfer-induced reactive oxygen species,” *Biomaterials*, vol. 124, pp. 25–34, 2017.

[14] M. N. Dickson, E. I. Liang, L. A. Rodriguez, N. Vollereaux, and A. F. Yee, "Nanopatterned polymer surfaces with bactericidal properties," *Biointerphases*, vol. 10, no. 2, p. 021010, 2015.
[15] T. Diu, N. Faruqui, T. Sjöström, B. Lamarre, H. F. Jenkinson, B. Su, and M. G. Ryadnov, "Cicada-inspired cell-instructive nanopatterned arrays," *Scientific reports*, vol. 4, p. 7122, 2014.
[16] J. Hasan, S. Raj, L. Yadav, and K. Chatterjee, "Engineering a nanostructured 'super surface' with superhydrophobic and superkilling properties," *RSC advances*, vol. 5, no. 56, pp. 44953–44959, 2015.
[17] F. D. Lowy, "Staphylococcus aureus infections," *New England journal of medicine*, vol. 339, no. 8, pp. 520–532, 1998.
[18] R. G. Bailey, R. D. Turner, N. Mullin, N. Clarke, S. J. Foster, and J. K. Hobbs, "The interplay between cell wall mechanical properties and the cell cycle in Staphylococcus aureus," *Biophysical journal*, vol. 107, no. 11, pp. 2538–2545, 2014.
[19] P. Eaton, J. C. Fernandes, E. Pereira, M. E. Pintado, and F. X. Malcata, "Atomic force microscopy study of the antibacterial effects of chitosans on Escherichia coli and Staphylococcus aureus," *Ultramicroscopy*, vol. 108, no. 10, pp. 1128–1134, 2008.
[20] S. Pogodin, J. Hasan, V. A. Baulin, H. K. Webb, V. K. Truong, V. Boshkovikj, C. J. Fluke, G. S. Watson, J. A. Watson, R. J. Crawford, and others, "Biophysical model of bacterial cell interactions with nanopatterned cicada wing surfaces," *Biophysical journal*, vol. 104, no. 4, pp. 835–840, 2013.
[21] J. S. Milner, M. W. Grol, K. L. Beaucage, S. J. Dixon, and D. W. Holdsworth, "Finite-element modeling of viscoelastic cells during high-frequency cyclic strain," *Journal of functional biomaterials*, vol. 3, no. 1, pp. 209–224, 2012.
[22] L. Wang, H.-Y. Hsu, X. Li, and C. J. Xian, "Effects of Frequency and Acceleration Amplitude on Osteoblast Mechanical Vibration Responses: A Finite Element Study," *BioMed research international*, vol. 2016, 2016.
[23] C. Hartmann, K. Mathmann, and A. Delgado, "Mechanical stresses in cellular structures under high hydrostatic pressure," *Innovative food science & emerging technologies*, vol. 7, no. 1–2, pp. 1–12, 2006.
[24] E. Zhou, C. Lim, and S. Quek, "Finite element simulation of the micropipette aspiration of a living cell undergoing large viscoelastic deformation," *Mechanics of Advanced Materials and Structures*, vol. 12, no. 6, pp. 501–512, 2005.
[25] G. Francius, O. Domenech, M. P. Mingeot-Leclercq, and Y. F. Dufrêne, "Direct observation of Staphylococcus aureus cell wall digestion by lysostaphin," *Journal of bacteriology*, vol. 190, no. 24, pp. 7904–7909, 2008.
[26] F. Xue, J. Liu, L. Guo, L. Zhang, and Q. Li, "Theoretical study on the bactericidal nature of nanopatterned surfaces," *Journal of theoretical biology*, vol. 385, pp. 1–7, 2015.
[27] Y. Jin, Y. Zhang, H. Ouyang, M. Peng, J. Zhai, and Z. Li, "Quantification of Cell Traction Force of Osteoblast Cells Using Si Nanopillar-Based Mechanical Sensor," *Sensors and Materials*, vol. 27, no. 11, pp. 1071–1077, 2015.
[28] S. Janbaz, N. Noordzij, D. S. Widyaratih, C. W. Hagen, L. E. Fratila-Apachitei, and A. A. Zadpoor, "Origami lattices with free-form surface ornaments," *Science advances*, vol. 3, no. 11, p. eaao1595, 2017.

[29] W. et al., “Towards osteogenic and bactericidal nanopatterns,” 2018.
[30] S. Wu, F. Zuber, J. Brugger, K. Maniura-Weber, and Q. Ren, “Antibacterial Au nanostructured surfaces,” *Nanoscale*, vol. 8, no. 5, pp. 2620–2625, 2016.
[31] J. J. Perry, J. T. Staley, S. Lory, and others, *Microbial life.* Sinauer Associates Incorporated, 2002.
[32] J. Thwaites and N. H. Mendelson, “Biomechanics of bacterial walls: studies of bacterial thread made from Bacillus subtilis,” *Proceedings of the National Academy of Sciences*, vol. 82, no. 7, pp. 2163–2167, 1985.
[33] F. Li, C. U. Chan, and C. D. Ohl, “Yield strength of human erythrocyte membranes to impulsive stretching,” *Biophysical journal*, vol. 105, no. 4, pp. 872–879, 2013.
[34] E. P. Ivanova, J. Hasan, H. K. Webb, G. Gervinskas, S. Juodkazis, V. K. Truong, A. H. Wu, R. N. Lamb, V. A. Baulin, G. S. Watson, and others, “Bactericidal activity of black silicon,” *Nature communications*, vol. 4, p. 2838, 2013.
[35] A. Tripathy, P. Sen, B. Su, and W. H. Briscoe, “Natural and bioinspired nanostructured bactericidal surfaces,” *Advances in colloid and interface science*, vol. 248, pp. 85–104, 2017.
[36] S. Kim, U. T. Jung, S.-K. Kim, J.-H. Lee, H. S. Choi, C.-S. Kim, and M. Y. Jeong, “Nanostructured multifunctional surface with antireflective and antimicrobial characteristics,” *ACS applied materials & interfaces*, vol. 7, no. 1, pp. 326–331, 2015.
[37] X. Li, “Bactericidal mechanism of nanopatterned surfaces,” *Physical Chemistry Chemical Physics*, vol. 18, no. 2, pp. 1311–1316, 2016.
[38] X. Li and T. Chen, “Enhancement and suppression effects of a nanopatterned surface on bacterial adhesion,” *Physical Review E*, vol. 93, no. 5, p. 052419, 2016.
[39] A. Mai-Prochnow, M. Clauson, J. Hong, and A. B. Murphy, “Gram positive and Gram negative bacteria differ in their sensitivity to cold plasma,” *Scientific reports*, vol. 6, p. 38610, 2016.
[40] M. T. Madigan and J. M. Martinko, “Microorganisms and microbiology,” *Brock biology of microorganisms. 11th ed. Upper Saddle River, New Jersey (NJ): Pearson Prentice Hall*, pp. 1–20, 2006.

Figure captions

Figure 1. a) A schematic drawing of *Staphylococcus aureus* and osteoblast and the dimensions used in our finite element models. b) The different parameters of nanopatterned structures including the height H, width, W, interspacing, IS, radius, r, and shape of the nanopillars. c) A schematic drawing displaying the positioning of the bacteria on nanopatterned structures.

Figure 2. The effects of different geometrical features including the (a) height, H, (b) interspacing, IS, (c) width, W, (d) shape, and (e) radius, r of the nanopillars on the sinking depth ratio, $\frac{SD}{D}$, and equivalent von Mises strain, ε_{eq}.

Figure 3. a) The results of four numerical simulations of how osteoblasts interact with nanopillars. The geometrical features of each model are presented in Table S3. b) Normalized equivalent von Mises strain, ε_{eq}, with respect to the rupture strain, ε_{th}. c) A map of bactericidal and cytotoxic behaviors predicted for different dimensions of the nanopillars. The interspace and width are normalized to the diameter of bacteria. The Log-log plots of von Misses strain versus two normalized parameters (d) $\frac{W}{W+IS}$ and (e) $\frac{R}{IS}$.

Figure 1

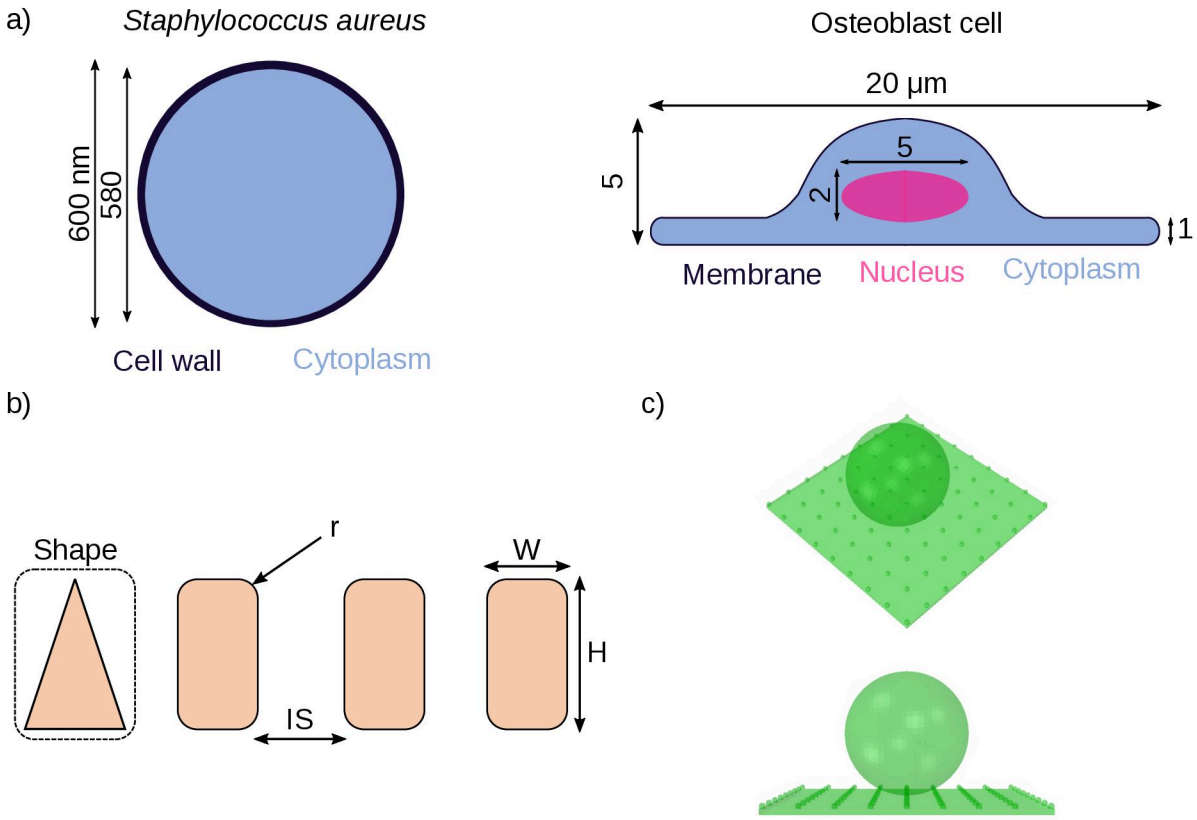
a)
Staphylococcus aureus
600 nm
580
Cell wall
Cytoplasm
Osteoblast cell
20 µm
5
5
2
1
Membrane
Nucleus
Cytoplasm
b)
Shape
r
W
H
IS
c)

Figure 2

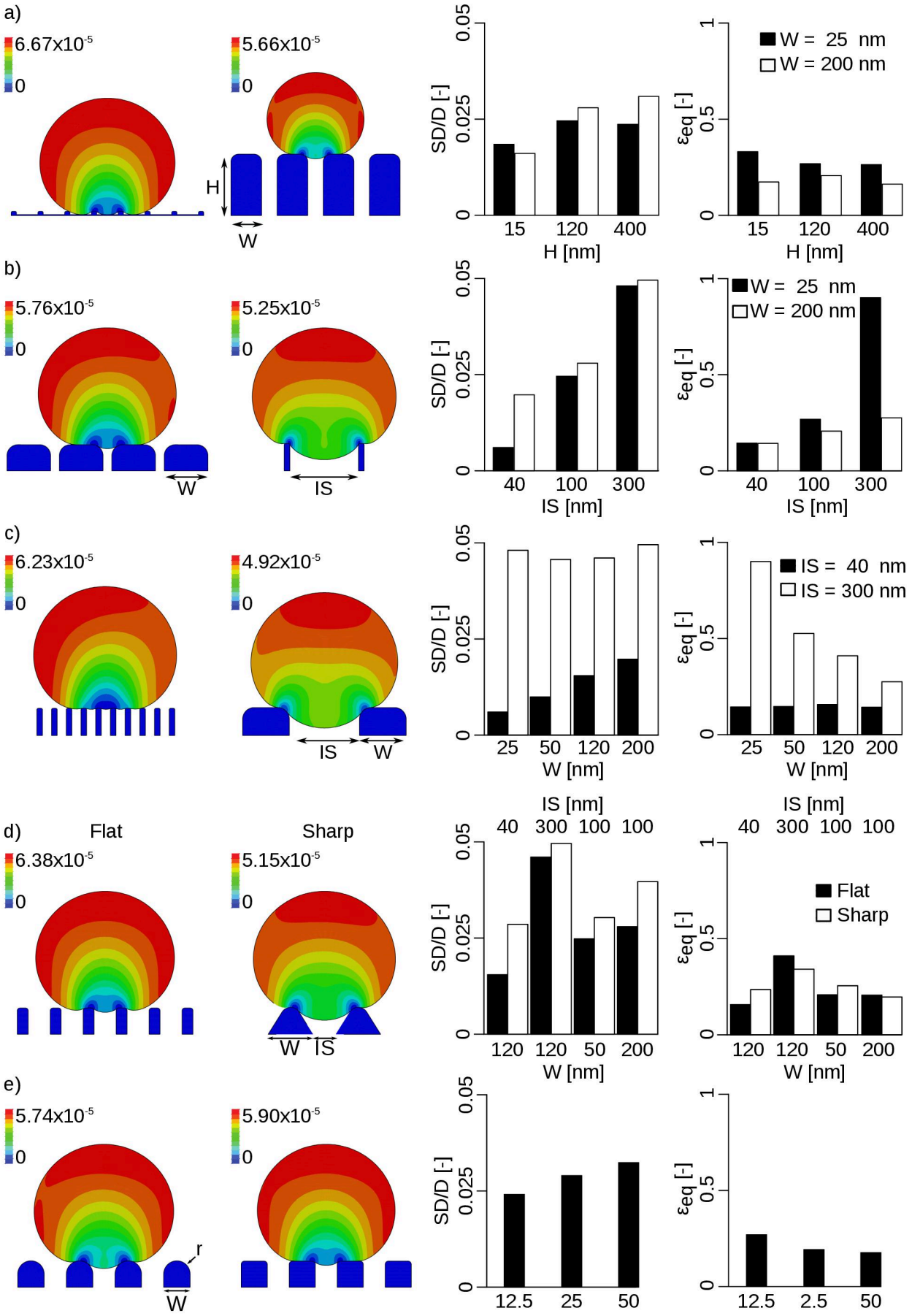
a)
6.67x10-5
0
5.66x10-5
0
H
W
SD/D [-]
0.05
0.025
0
15
120
400
H [nm]
W = 25 nm
W = 200 nm
εeq [-]
1
0.5
0
b)
5.76x10-5
0
5.25x10-5
0
W
IS
40
100
300
IS [nm]
c)
6.23x10-5
0
4.92x10-5
0
IS
W
25
50
120
200
W [nm]
IS = 40 nm
IS = 300 nm
d)
Flat
Sharp
6.38x10-5
0
5.15x10-5
0
W
IS
e)
5.74x10-5
0
5.90x10-5
0
r
W
12.5
25
50
2.5

Figure 3

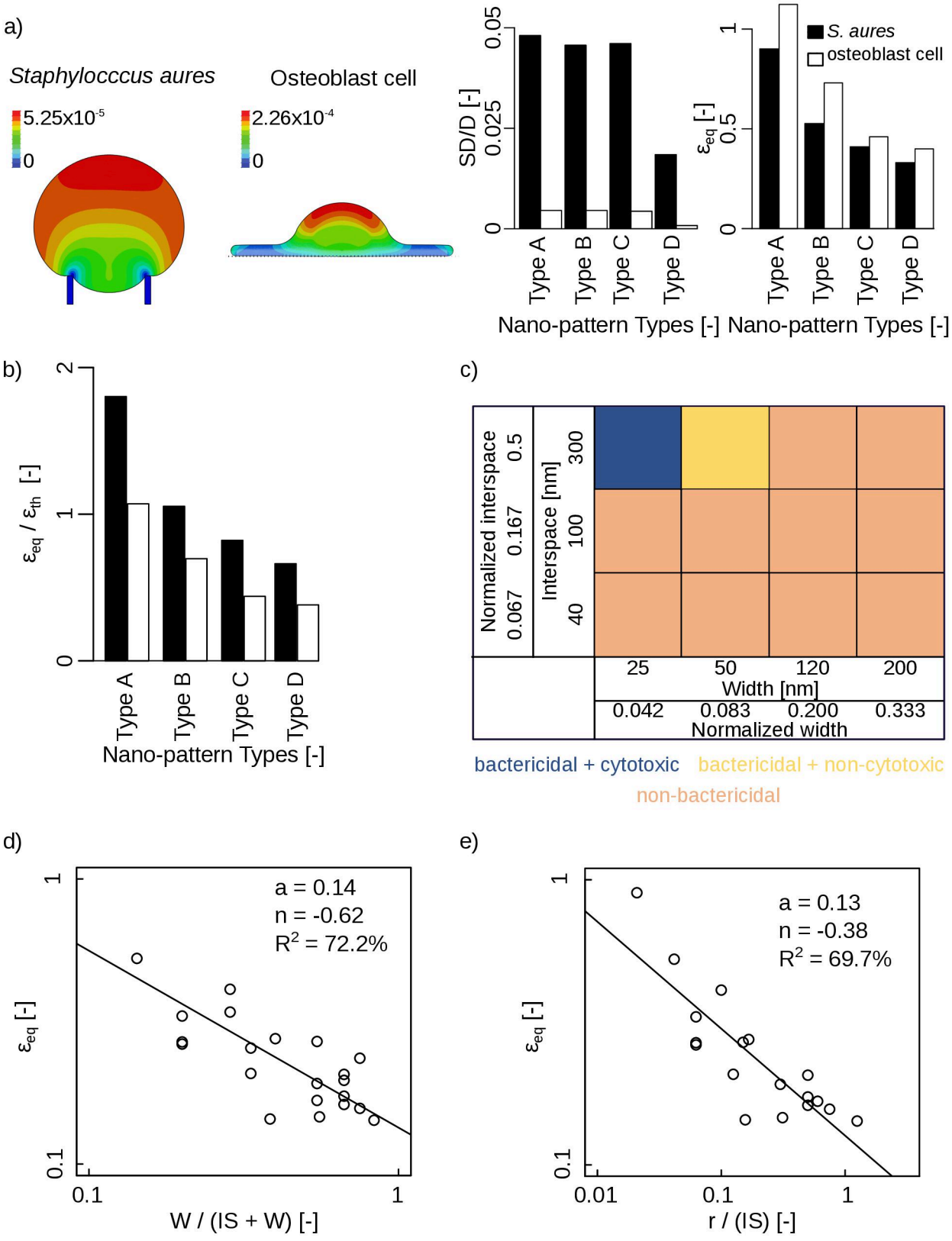
a)
Staphylocccus aures
Osteoblast cell
5.25x10-5
0
2.26x10-4
0
SD/D [-]
0.05
0.025
0
εeq [-]
1
0.5
0
S. aures
osteoblast cell
Type A
Type B
Type C
Type D
Nano-pattern Types [-]
Nano-pattern Types [-]
b)
εeq / εth [-]
2
1
0
Type A
Type B
Type C
Type D
Nano-pattern Types [-]
c)
Normalized interspace
0.5
0.167
0.067
Interspace [nm]
300
100
40
25
50
120
200
Width [nm]
0.042
0.083
0.200
0.333
Normalized width
bactericidal + cytotoxic
bactericidal + non-cytotoxic
non-bactericidal
d)
a = 0.14
n = -0.62
R2 = 72.2%
εeq [-]
1
0.1
0.1
1
W / (IS + W) [-]
e)
a = 0.13
n = -0.38
R2 = 69.7%
εeq [-]
1
0.1
0.01
0.1
1
r / (IS) [-]